

Influence of doping with Co, Cu, Ce and Fe on structure and photocatalytic activity of TiO₂ nanoparticles

DAMIAN WOJCIESZAK*, MICHAL MAZUR, DANUTA KACZMAREK, JAROSLAW DOMARADZKI

Faculty of Microsystem Electronics and Photonics, Wrocław University of Science and Technology,
Janiszewskiego 11/17, 50-372 Wrocław, Poland

In this paper, structural and photocatalytic properties of TiO₂ nanopowders doped with 1 at.% of cerium, cobalt, copper and iron have been compared. Nanoparticles were synthesized by sol-gel technique and characterized by SEM, EDS and XRD methods. Moreover, their photocatalytic activity was determined based on decomposition of methyl orange. Results were compared with undoped powder. The structural investigations have revealed that all prepared nanopowders were nanocrystalline and had TiO₂-anatase structure. The average size of crystallites was ca. 4 nm to 5 nm. The distribution of the dopant was homogenous in case of all manufactured powders. Moreover, for TiO₂ doped with Co, Ce and Cu, aggregation effect was not as large as for TiO₂:Fe. The results of photocatalytic decomposition showed that self-cleaning activity of all prepared nanopowders was higher as compared to undoped one. Due to the efficiency of these reactions (after 5 hours) nanopowders can be ordered as: TiO₂:Co > TiO₂:Ce > TiO₂:Cu > TiO₂:Fe > TiO₂.

Keywords: TiO₂, Co, Ce, Cu, Fe, photocatalysis

1. Introduction

Decomposition of harmful compounds is a very crucial ecological problem. According to current knowledge, photocatalysis is an effective way of pollutants neutralization from the environment [1–8]. Many materials can be called as photocatalysts, but titanium dioxide is the undisputed leader in this domain [9–16]. TiO₂ can be used in many different forms (e.g. coatings or nanoparticles), but its photocatalytic efficiency depends from the active surface area, which in case of nanopowders is much higher as-compared to thin-film coatings [17]. Photocatalytic activity of TiO₂ is related to many factors and can be increased in several ways, one of which is doping with different elements [18–27]. However, we cannot say that each dopant added into TiO₂ will increase its activity. According to literature [28–30] ions of a suitable dopant introduce additional energy levels into TiO₂ band structure. They trap charge carriers in order to suppress band-to-band recombination. Moreover,

they also release these trapped carriers via thermal transition in order to receive a high number of effective charge carriers. The crucial is to choose the appropriate amount of the dopant. Based on the data reported in the literature, e.g. by Khalid et al. [26] or Bokare et al. [27] and also our previous work [31], it can be assumed with high probability that 1 at.% of the dopant is a quite good value for the photocatalysis. Although, according to Chang et al. [28], this issue is also attributed to the size of the photocatalyst. Suitable amount of the dopant and small sacrifices in charge carriers will reduce the carrier density in the bands. In consequence, band-to-band relaxation and diffusion of charge carriers to the surface will be inhibited. According to the literature [28, 32], the optimal amount of the dopant for the highest photocatalytic performance is particle-size dependent. The model of Bloh et al. [32] indicates that optimum amount of the dopant is inversely proportional to the particles size. It is worth to notice that in case of large particles, the high amount of the dopant is disadvantageous, because it results in more defect-mediated recombination during

*E-mail: damian.wojcieszak@pwr.edu.pl

transfer of the carriers to the surface [28, 33–35]. The carriers trapped in the quantum-sized particles are able to reach the interface, because their wave function spreads over entire aggregates of the photocatalyst, so the cancel effect can occur inside the nanoparticles [28, 30].

It is a fact, that each dopant will have a different influence on the properties of titanium dioxide due to its energy levels, coordination number and electronegativity [28]. In this work, Co, Ce, Cu and Fe were added into TiO₂ matrix and their influence on the structure, particles size and photocatalytic activity of TiO₂ was studied. Such choice of dopants and their amount (1 at.%) was preceded by a review of the literature [26–28, 36, 37]. Addition of these dopants should increase photocatalytic activity of titanium dioxide. For example, as it was reported by Xu *et al.* [38], Cu³⁺ ions can improve the activity of TiO₂ nanoparticles. Choi *et al.* [30] has revealed that the same will happen with Fe³⁺, whereas Co³⁺ ions may give opposite effect. According to Inturia *et al.* [36] incorporation of iron into TiO₂ matrix results in more efficient conversion in the visible light region whereas, doping with Ce, Co or Cu will work vice versa. Although, Sadanandam *et al.* [39] have shown that Co²⁺ ions can expand the photo-response of titanium dioxide into visible light region, they also have revealed that photocatalytic efficiency of TiO₂:Ce is the highest when amount of the dopant is 1 at.%. As it was described in the literature [37], the size of the crystallites in Co-doped TiO₂ is smaller than in case of undoped one, which suggests that cobalt has an inhibiting role on the growth of crystallites.

Doping TiO₂ with Ce, Co, Cu and Fe gives different results, because it is related to the preparation method and depends from the location of ions of these dopants in the structure of titanium dioxide. According to the literature [28], ions of Fe or Cu can be substituted at Ti⁴⁺ sites within TiO₂ due to similar ionic radii to Ti⁴⁺ (0.645 Å), while Co and Ce ions most likely will be located in interstitial positions due to high difference between ionic radii. However, Ce ions can be larger than TiO₂ pore diameter, so it is more possible to find them as

dispersed oxides on the surface of nanocrystals than incorporated in its lattice [36].

As it was described in the literature [28], ions of dopants that have high oxidation states decrease the energy of maximum and minimum of TiO₂ valence and conduction band, respectively. It is the result of oxygen deficiency for charge compensation. The high occupancy of d-orbital decreases energy of d-states, thus moving the energy levels away from the conduction band and contributing to the maximum of the valence band. According to [35], Fe³⁺ ions increase titanium dioxide band-edge energy due to introduction of localized Fe_(3dx²-y²) states to the maximum of TiO₂ valence band. Moreover, delocalized Ti⁴⁺/Fe_(3dz²)³⁺ states (occupied with electrons) are located at the level of 0.5 eV to 0.8 eV above the maximum of valence band, while the localized Fe_(3dxy)³⁺ and delocalized Ti⁴⁺/Fe_(3dxz/3dyz)³⁺ (unoccupied) states are positioned 0.7 eV below the maximum of TiO₂ conduction band [40]. In case of Fe²⁺ ions there is a lower oxidation number and bigger ionic radii than for Fe³⁺ (0.78 Å and 0.65 Å, respectively). This results in a shift of the maximum of TiO₂ valence band and energy states of Fe²⁺ to higher values. As it was described in the literature [28], due to completely filled d-orbitals, Cu⁺ ions have low potential of d-states. Delocalized Ti⁴⁺/Cu_(3dz²)⁺ and localized Cu_(3dx²-y²)⁺ states dominate the maximum of valence band of TiO₂:Cu and increase its band-edge [40, 41]. Energy levels of Cu²⁺ are similar to Cu⁺ in the band structure [41, 42]. In case of cerium, incorporation of its ions at 4+ state into titanium dioxide results in occurrence of unoccupied 4f states located at 1.5 eV below the minimum of conduction band [43, 44]. For TiO₂ doped with cobalt, the tolerance of its structure can be related to the local environment of Ti [37]. The difference between the ionic radii of Co ions (i.e. at 2+ state: 0.745 Å) and Ti⁴⁺ (0.605 Å) suggests that the solubility of cobalt in titanium dioxide will be dependent from the mechanism of charge compensation [45]. Usually, when cobalt is added to TiO₂ it is inserted at 2+ state, which results in distortion of its structure, because smaller Ti⁴⁺ ion is

replaced by larger-sized Co²⁺ [46]. This effect is directly connected with introduction of oxygen vacancies to preserve charge neutrality [37].

2. Experimental

Nanopowders based on TiO₂ were prepared by sol-gel technique [31]. For the synthesis, 75 mL of distilled water (pH = 1, adjusted with nitric acid, Baker, 65 %, d = 1.40 g/mL) was added dropwise to 2 mL of titanium tetraisopropoxide (TTIP, Sigma Aldrich, ≥ 98 %, d = 0.96 g/mL). Next, the solution was dissolved in 25 mL of 2-propanol (Lab-Scan, ≥ 99.7 %, d = 0.78 g/mL) under vigorous magnetic stirring and simultaneously heated at 80 °C for 6 hours. The process of hydrolysis of titanium precursor occurred immediately. In consequence, transparent colloidal system (with milky-like color) with TiO₂ concentration of about 5 g/L was obtained. Then, this solution was dried in an ambient air atmosphere at 120 °C for 2 hours. Thanks to that, white powder was obtained. Ce, Co, Cu and Fe doped TiO₂ nanoparticles were prepared using an appropriate amount of pure metal salts: (NH₄)₂Ce(NO₃)₆ (36.7 mg), CoCl₂·6H₂O (15.9 mg), Cu(NO₃)₂·3H₂O (16.1 mg) and FeCl₃ (10.9 mg). They were added in order to obtain a doping level of 1 at.%.

Structural properties of synthesized nanoparticles were determined based on the results of the X-ray diffraction (XRD) method. For the measurements, Siemens 5005 powder diffractometer with CoK α X-ray ($\lambda = 1.78897 \text{ \AA}$) was used. The XRD studies were performed using Co lamp filtered by Fe (30 mV, 25 mA), step size was equal to 0.02° in 2 θ range, while time-per-step was 5 s. The correction for the broadening of the XRD instrument was accounted and the crystallite sizes were calculated using Scherrer equation.

The surface morphology of thin films was investigated with the aid of a FESEM FEI Nova NanoSEM 230 scanning electron microscope (SEM) with 30 kV of acceleration voltage. Moreover, this system was equipped with EDAX EDS microanalyzer for investigation of material composition. Thanks to these experiments, maps with distribution of elemental composition were received.

The influence of doping TiO₂ with Ce, Co, Cu or Fe on its photocatalytic properties was estimated based on methyl orange (MO) decomposition. The experimental setup consisted of a UV-Vis light source ($P_{UV} = 183 \text{ W/m}^2$, $P_{Vis} = 167 \text{ W/m}^2$) and quartz-glass reservoir, which contained 200 mL of solution with MO concentration of 10 ppm and 50 ppm of the photocatalyst. The temperature of reaction was stabilized by circulation of water through a jacket at a constant temperature of ca. 15 °C. All experiments were carried out under agitation with a magnetic stirrer (700 rpm) in order to provide homogeneous concentration of the suspension in entire volume. In the experiment any external oxygen supply was used. To exclude the self-decomposition possibility of the used dye under illumination a blank experiment (in the absence of TiO₂) was carried out. The results have shown that the decomposition of MO in the absence of nanopowders was not observed or the rate of this reaction was very low. Moreover, 30 minutes of premixing at a constant temperature in a dark condition was enough to achieve an adsorption/desorption equilibrium and after that time, the light was switched on to initiate the reaction. To determine the change in MO concentration, the samples containing its solutions were withdrawn from the reactor regularly every 60 minutes for 5 hours. The solutions were analyzed by OceanOptics QE 65000 UV-Vis spectrophotometer coupled with Mikropack DH-2000-BAL deuterium-halogen light source, in the wavelength range of 300 nm to 700 nm. MO concentration was calculated from the absorption peak at ca. 466 nm by means of a calibration curve.

3. Results and discussion

The composition of prepared nanoparticles was determined by energy dispersive spectroscopy (EDS). It was found that the amount of cerium, cobalt, copper or iron was in quite good agreement to the base assumptions and it was c.a. 1 at.%. Moreover, the results of X-ray microanalysis (Fig. 1) have revealed, that the distribution of material composition (Ti, O and Ce, Co, Cu or Fe) was homogenous for all the nanopowders.

It is worth to notice that the concentration of the dopants was also homogenous and aggregation effect of Ce, Co, Cu or Fe (most probably in oxide forms) was not observed. However, due to low spatial resolution of EDS method the aggregation effect in nanoscale cannot be excluded. According to our previous works [26, 31] we believe that ions of these dopants are located on the surface of TiO_2 nanocrystals and they create their own oxide forms. Such location has a positive impact on energy transfer of photogenerated charge carriers during photocatalytic reaction [26].

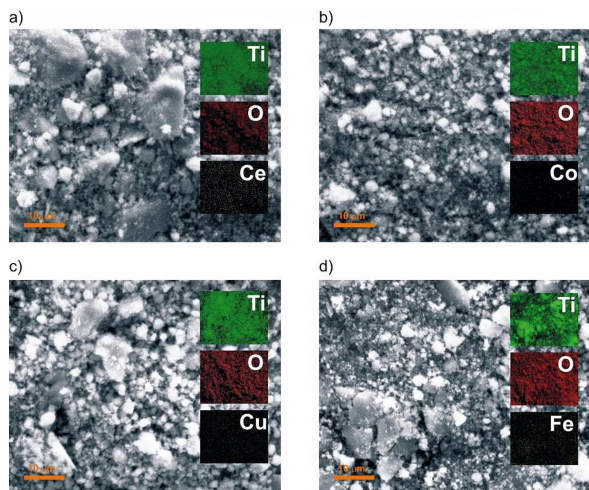


Fig. 1. The results of X-ray microanalysis of prepared nanopowders: (a) TiO_2 :Ce, (b) TiO_2 :Co, (c) TiO_2 :Cu, (d) TiO_2 :Fe. Secondary electron images of selected areas contain suitable images of the elements concentration distribution for: Ti, O and Ce, Co, Cu or Fe, respectively (area of investigation: ca. $50 \mu\text{m} \times 65 \mu\text{m}$).

Structural investigation also included an analysis of the morphology. SEM images obtained for the prepared nanoparticles (Fig. 2) have shown that all of them formed aggregates. However, it can be observed that their shapes and sizes were irregular. The most fine structure had TiO_2 doped with cobalt, but also TiO_2 :Ce and TiO_2 :Cu nanopowders had quite similar and very fine form of their morphology. In case of these powders small aggregates were present. A slightly different form had the undoped nanopowder and the one with iron, where the presence of large aggregates is very evident (Fig. 2e). Moreover, the shape and size of

TiO_2 and TiO_2 :Fe nanoparticles is not so uniform as-compared to TiO_2 :Ce, TiO_2 :Cu (Fig. 2b and Fig. 2d) or especially to TiO_2 :Co (Fig. 2c). Similar conclusions have been described also in literature and such effect can be obtained not only in case of change of the type of the dopant, but it can be a consequence of an appropriate selection of its amount [27, 31].

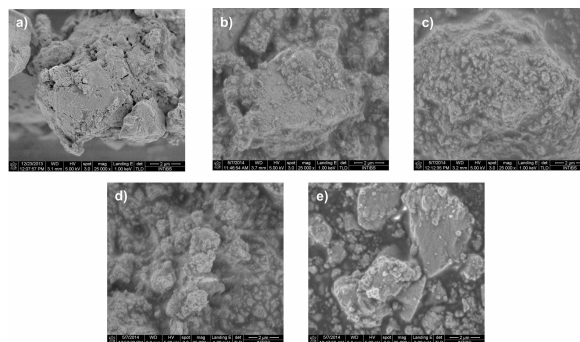


Fig. 2. SEM images of: (a) TiO_2 , (b) TiO_2 :Ce, (c) TiO_2 :Co, (d) TiO_2 :Cu, (e) TiO_2 :Fe nanopowders.

The structure of as-prepared nanopowders was determined based on XRD results. In Fig. 3 recorded patterns are presented, while in Table 1 parameters calculated on their base are collected. It was found that all prepared powders had well crystallized anatase structure. Moreover, all of them were nanocrystalline. For all samples reflections from (1 0 1), (0 0 4), (2 0 0) and (2 1 1) anatase crystal planes were observed. The average size of crystallites (calculated for (1 0 1) plane) was in the range of 4.1 nm to 5.0 nm. The largest crystallites (5 nm) were obtained in case of titanium dioxide nanopowder doped with Ce, while the lowest ones were in the sample doped with iron (4.1 nm). Due to low amount of the dopants their crystal forms have not revealed in the patterns. However, this does not exclude that such oxides, like e.g. Ce_2O_3 , CuO , CoO or Fe_2O_3 , occur in the surrounding of anatase nanocrystals.

Photocatalytic properties of the prepared nanopowders were determined on the basis of the MO decomposition under UV-Vis light exposure. The level of activity of titanium dioxide doped with Ce, Co, Cu and Fe was compared with

Table 1. Structural parameters of TiO₂ nanoparticles doped with 1 at.% of Ce, Co, Cu or Fe, based on XRD results.

Nanoparticles	Phase	(h k l)	2θ	d [nm]	d _{PDF} [nm]	D [nm]
TiO ₂	anatase	(1 0 1)	29.59	0.3503	0.3520 [47]	4.2
TiO ₂ :Ce			29.60	0.3502		5.0
TiO ₂ :Co			29.62	0.3500		4.1
TiO ₂ :Cu			29.64	0.3497		4.7
TiO ₂ :Fe			29.69	0.3491		4.1

Designations: d – interplanar distance, d_{PDF} – standard interplanar distance, D – average crystallites size

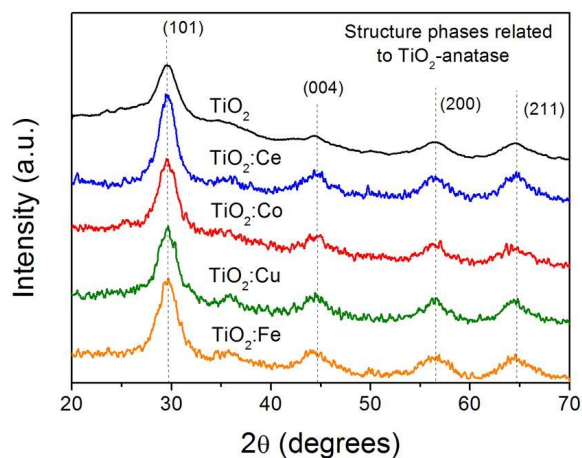


Fig. 3. XRD patterns of TiO₂, TiO₂:Ce, TiO₂:Co, TiO₂:Cu and TiO₂:Fe nanopowders.

the activity of undoped photocatalyst. It was found that all the nanopowders were characterized by a high photocatalytic activity. According to Fig. 4 it can be concluded that doping titanium dioxide with cobalt allowed us to obtain the most active photocatalyst. After 5 hours of the reaction carried out in presence of TiO₂:Co, 96 % of the dye was decomposed. Slightly lower activity was obtained in case of titanium dioxide doped with Ce and Cu. For these nanoparticles, after 5 hours in the solution 11 % and 12 % of methyl orange still remained. It can be concluded that their photocatalytic activity was the same. Titanium dioxide doped with iron was less active, because only c.a. 76 % of the dye was decomposed. However, this result is still better as compared to the activity of TiO₂, where after 5 hours of irradiation of the solution, 27 % of MO was left in the reactor. Moreover, comparing the decomposition rates

of the dye it can be noticed that for TiO₂ doped with Co, Ce and Fe, the reaction was still dynamic even at the end of the exposure time (after three hour), while in case of TiO₂:Cu some saturation effect occurred. Concluding, the activity of prepared nanopowders can be ordered as follows: TiO₂:Co > TiO₂:Ce > TiO₂:Cu > TiO₂:Fe > TiO₂ (order related to results after 5 hours of decomposition). We suggest that high activity of the prepared powders was connected with small size of the particles, which were in range of c.a. 4.1 nm to 5 nm. Thanks to that, very large surface active area per gram, especially for TiO₂:Co, TiO₂:Ce and TiO₂:Cu, was obtained. Moreover, as it is shown in the SEM images (Fig. 2), in case of these photocatalysts, aggregation effect did not occur in such high degree as it was observed for TiO₂ and TiO₂:Fe.

In our opinion, the role of ions of these dopants is beneficial in the energy transfer mechanism. Our previous works [25, 31, 48] have shown that the mechanisms of charge transport in titanium dioxide depends directly from the type of the dopant, its form (metallic or oxide one) and location (in the lattice or e.g. on the surface of TiO₂ nanocrystals). In case of as-prepared Ce, Co, Cu and Fe-doped TiO₂ nanopowders, the ions of these dopants participate in the direct or indirect transfer of excited electrons from the conduction band of the matrix (titanium dioxide), via or without its defect levels, respectively. The dopants were located probably on the surface of TiO₂ nanoparticles. This is indicated by XRD studies that have not revealed the occurrence of stress in the crystal lattice of TiO₂ (measured and standard interplanar spacing are similar in all cases). Thanks to such so called ‘surface

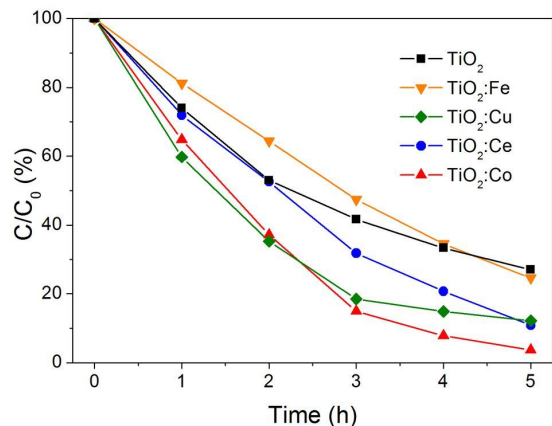


Fig. 4. Comparison of photocatalytic activity of TiO₂ nanopowders doped with 1 at.% of Ce, Co, Cu and Fe as-compared with TiO₂, after exposure to the UV-Vis light. Designations: C₀ – initial concentration and C – concentration of methyl orange after time t.

doping' ions of all dopants are involved in charge trapping, recombination and interfacial transfer.

According to work [28], usually higher number of the trapped holes in the Fe-doped samples shows that interfacial charge transfer from the conduction band to the adsorbed oxygen molecules is more efficient than the lattice trapping by the dopants. Our experiment has shown that TiO₂:Fe nanopowder had the lowest activity. Probably it stems from the fact that charge recombination process occurred too fast to allow interfacial transfer. As it was reported in the literature [28] this effect consumes a substantial number of effective charge carriers. An opposite effect was observed for TiO₂ doped with Co. As it was mentioned, cobalt usually occurs in TiO₂ at 2+ state. Due to its smaller ionic radius as-compared to Ti⁴⁺ it may replace this ion and introduce oxygen vacancies, but it depends also from the local environment of titanium [37, 49]. We suggest that cobalt occurred in CoO form among TiO₂ grain boundaries and thanks to that such high photocatalytic activity has been obtained. According to work [30], presence of Co³⁺ ions would decrease the activity of titanium dioxide so their presence is rather unlikely. In case of TiO₂ doped with Ce and Cu, these ions can provide alternative pathways for energy transfer

on the surface of TiO₂ nanoparticles (they can trap carriers in order to interact with the adsorbates), what results in an increase in photocatalytic activity of such powders [28, 30]. Moreover, due to location of copper ions on the surface of nanocrystals, the stabilization effect of photo-generated electrons and holes can occur [28]. This has a positive impact on the efficiency of energy transfer and photocatalytic activity of TiO₂:Cu. In our opinion, the same effects occurred in case of our TiO₂ nanopowders doped with 1 at.% of cooper. As regards to TiO₂:Ce, there are some reports, which testify that cerium reduces the activity of titanium dioxide because its ions act as recombination centers, but they can also inhibit the recombination via charge separation [50, 51]. Usually, the low activity of such films is obtained when cerium occurs in metallic form and its ions severe as recombination centers [52]. However, when cerium ions at 4+ state are located on the surface of TiO₂ there is an opposite effect. Ce⁴⁺ ions strongly bind the chemisorbed oxygen radicals on the surface, thus inhibiting the interaction of these radicals with the trapped holes [28]. We suggest that similar process took place in case of our powder.

4. Conclusions

In this paper, structural and photocatalytic properties of nanocrystalline titanium dioxide nanopowders doped with 1 at.% of cerium, cobalt, cooper and iron have been presented. All samples prepared by sol-gel technique had TiO₂-anatase structure, and the average size of their crystallites was ca. 4 nm to 5 nm. The distribution of used dopant was homogenous for all manufactured powders. Moreover, in case of TiO₂ doped with Co, Ce and Cu, aggregation effect was not as high as for TiO₂:Fe or undoped TiO₂. The results of photocatalytic decomposition showed that self-cleaning activity of all prepared nanopowders was higher as compared to undoped one. Due to the efficiency of these reactions (after 5 hours) nanopowders can be ordered as: TiO₂:Co > TiO₂:Ce > TiO₂:Cu > TiO₂:Fe > TiO₂.

Acknowledgements

This work was financed from the MNiSW within the Iuventus Plus program (no. IP2014 051673) and statutory sources in 2016-2017 years (zlec. 0402/0183/16).

References

- [1] FUJISHIMA A., RAO T.N., TRYK D.A., *J. Photoch. Photobio. C*, 1 (2000), 1.
- [2] FOX M.A., DULAY M.T., *Chem. Rev.*, 83 (1995), 341.
- [3] THOMPSON T.L., YATES J.T., *Chem. Rev.*, 106 (2006), 4428.
- [4] FIJISFIMA A., ZHANG X., *Comptes. Rendus. Chimie.*, 9 (2006), 750.
- [5] CHEN X., MAO S.S., *Chem. Rev.*, 107 (2007), 2891.
- [6] SERPONE N., PELIZETTI E., *Wiley*, (1989).
- [7] SCHIAVELLO M., *Kluwer Academic Publishers*, (1988).
- [8] SCHIAVELLO M., *John Wiley & Sons* 3, (1997).
- [9] LEE S., ROBERTSON P.K.J., MILLS A., McSTAY D., *J. Photoch. Photobio. A.*, 122 (2010), 69.
- [10] CHOI W., *Catal. Surv. Asia*, 10 (2006), 16.
- [11] FERNANDEZ-GARCIA M., MARTINEZ-ARIAS A., HANSON J.C., RODRIGUEZ J.A., *Chem. Rev.*, 104 (2004), 4063.
- [12] BURNS A., HAYES G., LI W., HIRVONEN J., DEMAREE J.D., SHAH I., *Mat. Sci. Eng. B-Adv.*, 111 (2004), 150.
- [13] CHEN L., GRAHAM M.E., LI G., GRAY K.A., *Thin Solid Films*, 515 (2006), 1176.
- [14] DOLAT D., MOZIA S., WRÓBEL R.J., MOSZYNSKI D., OHTANI B., GUSKOS N., MORAWSKI A.W., *Appl. Catal. B-Environ.*, 162 (2015), 310.
- [15] BUBACZ K., CHOINA J., DOLAT D., BOROWIAK-PALEN E., MOSZYNSKI D., MORAWSKI A.W., *Mater. Res. Bull.*, 45 (2010), 1085.
- [16] JANUS M., MORAWSKI A.W., *Appl. Catal. B-Environ.*, 75 (2007), 118.
- [17] GAYA U.I., ABDULLAH A.H., *J. Photoch. Photobio. C-Photoch. Rev.*, 9 (2008), 1.
- [18] JING L., SUN X., XIN B., WANG B., CAI W., FU H., *J. Solid State Chem.*, 177 (2004), 3375.
- [19] KIM H.R., LEE T.G., SHUL Y.G., *J. Photoch. Photobio. A-Chem.*, 185 (2007), 156.
- [20] LIQIANG J., YICHUN Q., BAIQI W., SHUDAN L., BAOJIANG J., LIBIN Y., WEI F., HONGGANG F., JIAZHONG S., *Sol. Energ. Mat. Sol. C.*, 90 (2006), 1773.
- [21] RENGARAJ S., VENKATARAJ S., YEON J.W., KIM Y., LI X.Z., PANG G.K.H., *Appl. Catal. B-Environ.*, 77 (2007), 157.
- [22] STENGL V., BAKARDJIEVA S., MURAFI N., *Mater. Chem. Phys.*, 114 (2009), 217.
- [23] XIE Y., YUAN CH., *Appl. Surf. Sci.*, 221 (2004), 17.
- [24] NAKAMURA I., NEGISHI N., KUTSUNA S., *J. Mol. Catal. A-Chem.*, 161 (2000), 205.
- [25] WOJCIESZAK D., KACZMAREK D., DOMARADZKI J., MAZUR M., *Int. J. Photoenerg.*, (2013), 1.
- [26] KHALID N.R., AHMED E., HONG Z., ZHANG Y., UL-LAH M., AHMED M., *Ceram. Int.*, 39 (2013), 3569.
- [27] BOKARE A., SANAP A., PAI M., SABHARWAL S., ATHAWALE A.A., *Colloid. Surface. B*, 102 (2013), 273.
- [28] CHANG S.M., LIU W.S., *Institute Appl. Catal. B-Environ.*, 156-157 (2014), 466.
- [29] LI J., XU J., DAI W.L., LI H., FAN K., *Appl. Catal. B-Environ.*, 85 (2009), 162.
- [30] CHOI W., TERMIN A., HOFFMANN M.R., *J. Phys. Chem.*, 98 (1994), 13669.
- [31] WOJCIESZAK D., MAZUR M., KURNATOWSKA M., KACZMAREK D., DOMARADZKI J., KEPIŃSKI L., CHOJNACKI K., *Int. J. Photoenerg.*, (2014), 1.
- [32] BLOH J.Z., DILLERT R., BAHNEMANN D.W., *J. Phys. Chem. C*, 116 (2012), 25558.
- [33] ZHANG Z., WANG C.C., ZAKARIA R., YING J.Y., *J. Phys. Chem. B*, 102 (1998), 10871.
- [34] ZHU J., CHEN F., ZHANG J., CHEN H., ANPO M., *J. Photoch. Photobiol. A-Chem.*, 180 (2006), 196.
- [35] ZHU J., DENG Z., CHEN F., ZHANG J., CHEN H., ANPO M., HUANG J., ZHANG L., *Appl. Catal. B-Environ.*, 62 (2006), 329.
- [36] INTURIA S.N.R., BONINGARA T., SUIDANB M., SMIRNIOTISA P.G., *Appl. Catal. B-Environ.*, 144 (2014), 333.
- [37] SAMET L., BEN NASSEUR J., CHTOUROU R., MARCH K., STEPHAN O., *Mater. Charact.*, 85 (2013), 1.
- [38] XU A.W., GAO Y., LIU H.Q., *J. Catal.*, 207 (2002), 151.
- [39] SADANANDAM G., LALITHA K., KUMARI V.D., SHANKAR M.V., SUBRAHMANYAM M., *Int. J. Hydrogen Energ.*, 38 (2013), 9655.
- [40] SHOUGH A.M., DOREN D.J., OGUNNAIKE B., *Chem. Mater.*, 21 (2009), 1232.
- [41] GUO M., DU J., *Physica B*, 407 (2012), 1003.
- [42] NAKAJIMA N., KATO H., OKAZAKI T., SAKISAKA Y., *Surf. Sci.*, 561 (2004), 93.
- [43] CHEN W., YUAN P., ZHANG S., SUN Q., LIANG E., JIA Y., *Physica B*, 407 (2012), 1038.
- [44] KAMISAKA H., SUENAGA T., NAKAMURA H., YAMASHITA K., *J. Chem. C*, 114 (2010), 12777.
- [45] PARMAR K.P.S., RAMASAMY E., LEE J.W., LEE J.S., *Scripta Mater.*, 62 (2010), 223.
- [46] KULJANIN-JAKOVLJEVIC J., RADOICIC M., RADETIĆ T., KONSTANTINOVIC Z., SAPONJIC Z.V., NEDELJKOVIC J., *J. Phys. Chem.*, 113 (2009), 21029.
- [47] Powder Diffraction File (1967). Joint Committee on Powder Diffraction Standards, Philadelphia, PA, Card No. 21-1272.
- [48] WOJCIESZAK D., KACZMAREK D., DOMARADZKI J., MAZUR M., MORAWSKI A.W., JANUS M., PROCIOW E., GEMMELLARO P., *Pol. J. Chem. Technol.*, 14 (2012), 1.
- [49] MAIRA A.J., CONESA J.C., YEUNG K.L., AUGUGLIARO V., SORIA J., CORONADO J.M., *Langmuir*, 17 (2001), 5368.
- [50] ZHU J., ZHENG W., HE B., ZHANG J., ANPO M., *J. Mol. Catal. A-Chem.*, 216 (2004), 35.

- [51] TONG T., ZHANG J., TIAN B., CHEN F., HE D., *J. Hazard. Mater.*, 155 (2008), 572.
- [52] CHEN H., CHEN S., QUAN X., YU H., ZHAO H., ZHANG Y., *J. Phys. Chem. C*, 112 (2008), 9285.

Received 2016-10-25

Accepted 2018-01-24